fluids

MDPI

Article

AI-Driven Optimization of Breakwater Design: Predicting Wave Reflection and Structural Dimensions

Mohammed Loukili [1], Soufiane El Moumni [2] and Kamila Kotrasova [3,*]

[1] Institut de Recherche de l'Ecole Navale (EA 3634, IRENav), 29160 Brest, France; mohammed.loukili@ecole-navale.fr
[2] Digital Engineering for Leading Technology and Automation Laboratory (DELTA Lab), Hassan II University of Casablanca, Casablanca 20670, Morocco; soufianeelmoumni@gmail.com
[3] Institute of Structural Engineering and Transportation Structures, Faculty of Civil Engineering, Technical University of Kosice, Vysokoskolska 4, 042 00 Kosice, Slovakia
* Correspondence: kamila.kotrasova@tuke.sk; Tel.: +421-55-602-4294

Abstract: Coastal defense structures play a crucial role in mitigating wave impacts; yet, existing breakwater designs often face challenges in balancing wave reflection, energy dissipation, and structural stability. This study leverages machine learning (ML) to predict the optimal 2D dimensions of rectangular breakwaters in two configurations: submerged at the bottom of a wave tank and positioned at the free surface. Further, the objective is to achieve controlled wave reflection allowing a specific wave run-up and optimized energy dissipation, while ensuring maritime stability. Thus, we used an analytical equation modeling the reflection coefficient versus relative water depth (KH), for different immersion ratios of obstacle (h/H), and relative length (l/H). Two datasets of 32,000 data points were generated for underwater and free-surface breakwaters, with an additional 10,000 data points for validation, totaling 42,000 data points per case. Five ML algorithms—Random Forest, Support Vector Regression, Artificial Neural Network, Decision Tree, and Gaussian Process—were applied and evaluated. Results demonstrated that Random Forest and Decision Tree balanced accuracy with computational efficiency, while the Gaussian Process closely matched analytical results but demanded higher computational resources. These findings support ML as a powerful tool to optimize breakwater design, complementing traditional methods and contributing to more sustainable and resilient coastal defense systems.

Keywords: machine learning (ML); breakwater design; wave reflection; maritime engineering; coastal defense

Academic Editor: Filippos Sofos

Received: 10 December 2024
Revised: 22 January 2025
Accepted: 27 January 2025
Published: 30 January 2025

Citation: Loukili, M.; El Moumni, S.; Kotrasova, K. AI-Driven Optimization of Breakwater Design: Predicting Wave Reflection and Structural Dimensions. *Fluids* **2025**, *10*, 34. https://doi.org/10.3390/fluids10020034

1. Introduction

Artificial intelligence (AI) has emerged as a transformative technology, revolutionizing multiple sectors by processing large datasets, recognizing patterns, and making data-driven decisions with minimal human intervention [1–4]. In the medical field, AI improves diagnostic accuracy and treatment plans through advancements such as medical image analysis [5], while deep learning techniques in computational hemodynamics enable non-invasive diagnostic methods and treatments for vascular conditions [6]. AI applications extend beyond healthcare and engineering, finding use in industrial optimization through computational fluid dynamics and numerical techniques to enhance efficiency

and reduce environmental impact in glass manufacturing [7]. Moreover, it supports pipeline integrity management by employing transient test techniques to detect partial blockages in pressurized systems [8] and facilitates the prediction of ionic liquid properties using machine learning approaches, offering a data-driven alternative to experimental procedures and molecular simulations [9]. In education, intelligent tutoring systems offer personalized learning experiences [10]. The maritime industry has seen significant advancements through AI, enhancing safety, efficiency, and sustainability [11]. AI-powered Autonomous Surface Vehicles (ASVs) use machine learning algorithms for real-time route optimization, collision avoidance, and obstacle detection, reducing human error [12–14]. Predictive maintenance systems analyze sensor data to forecast equipment failures, minimizing downtime and maintenance costs [15]. For instance, reduced-order CFD models have been developed to support wind turbine maintenance by accurately assessing the impact of leading-edge erosion on blade performance, enabling precise maintenance planning [16]. Additionally, AI-driven weather routing systems optimize fuel usage and contribute to eco-friendly shipping practices [17]. As AI continues to evolve, its potential for transforming maritime operations and other industries remains substantial, positioning it as a critical tool for addressing complex challenges and driving innovation.

The focus of our scientific work is to leverage machine learning (ML) to predict the optimal 2D dimensions of rectangular breakwaters. Two cases are treated in this work: underwater breakwater and free-surface breakwater. For the sake of clarity, accurate prediction of breakwater dimensions is crucial for balancing and controlling wave reflection, energy dissipation, and structural stability. By modeling these interactions using machine learning, the researchers and engineers will be able to optimize the structure's performance in terms of energy dissipation, ensuring the desired outcomes of wave behavior. For more clarity, this is a continuation of our research work cited in the reference [18].

Extensive research has been conducted on various types of breakwaters. However, due to the complex operating conditions of breakwaters, further studies are needed to address existing knowledge gaps. A brief summary of past work is provided here. Dean [19] explored how wave amplitudes affect the reflection of surface waves by a submerged flat barrier. Takano [20] examined the effect of waves passing beneath a rectangular breakwater. Patarapanich [21] investigated wave reflection and transmission using the finite element method (FEM) on a submerged thin horizontal plate. Liu and Jiankng [22] used the matched asymptotic method to study wave transmission through a submerged slit on a vertical barrier. Stamos et al. [23] employed parametric experiments to compare reflection and transmission coefficients from waves interacting with different submerged water-filled breakwater models of hemi-cylindrical and rectangular shapes. Molin et al. [24] conducted lab experiments on wave interaction with a rigid vertical plate, followed by Lui et al. [25], who studied Bragg reflections caused by waves on multiple submerged semi-circular breakwaters.

The submerged rectangular step is commonly used as a breakwater to shield shorelines, mitigate wave damage, reduce coastal erosion, and protect coastal structures [26]. Recently, submerged rectangular breakwaters have gained more attention than traditional emerged structures due to their esthetic appeal, ability to promote water circulation, and allow fish passage. Numerous experimental, analytical, and numerical studies have investigated wave reflection and transmission in relation to these structures. Mei and Black [27] used the variational method to study the scattering properties of bottom and surface obstacles. Massel [28] analyzed wave interaction with rectangular submerged breakwaters of infinite and finite lengths. Andrew et al. [29] conducted experimental and numerical research using the boundary element method (BEM) to explore wave propagation over a submerged rectangular impermeable obstacle. More recently, Szmidt [30] used the finite

difference method (FDM) to numerically assess wave interaction with a rectangular breakwater fixed to the bottom of a numerical wave tank, evaluating its effectiveness in protecting coastal shelf zones from open sea waves.

Nowadays, the application of artificial intelligence (AI) to predict optimal breakwater dimensions has gained significant attention. Machine learning (ML) models have been used to predict wave reflection and transmission based on varying breakwater geometries. For example, in [31,32], the authors applied Artificial Neural Network (ANN) to model wave-structure interactions, allowing the prediction of optimal breakwater dimensions with minimal computational effort. Similarly, the work by MAO et al. demonstrated the use of genetic algorithms to optimize the geometry of submerged breakwaters, effectively reducing wave energy [33]. These AI-driven approaches provide a more efficient and accurate way to determine the optimal breakwater dimensions for desired wave reflection and transmission coefficients, offering a powerful tool for engineers working on maritime structure design.

The cited articles, while innovative, exhibit several limitations that open the door for further research and improvement. For instance, the authors in [31,32] focused primarily on neural networks but did not extensively explore the generalization capabilities of their model to different wave conditions or more complex breakwater shapes. The model's predictive accuracy under non-regular or irregular waves remains under-explored, which could limit its application in real-world, unpredictable maritime environments. Moreover, MAO et al. used genetic algorithms to optimize submerged breakwater geometries, but their method faced challenges in terms of computational complexity and convergence speed [33]. The algorithm's efficiency in handling high-dimensional design spaces or incorporating multiple environmental factors simultaneously is still an area of concern. These limitations highlight the need for more robust, scalable, and flexible AI models capable of handling a broader range of scenarios, including varying wave conditions and more complex geometries, which will be the focus of the work presented in this paper.

In addition, while previous works primarily focused on single algorithms or optimization techniques, our research aims to overcome this by presenting and comparing five different machine learning algorithms to predict the optimal dimensions of the breakwater. This approach allows for a more comprehensive evaluation and deeper comparison, helping to identify the most suitable algorithm for this specific problem. By doing so, we address the need for a more flexible and accurate predictive model that can adapt to varying wave conditions and geometric complexities, ultimately improving the reliability and efficiency of breakwater design in real-world scenarios.

This paper is structured as follows: Section 2 outlines the problem formulation and the adopted methodology, providing the foundation for the analysis. Section 3 presents the results and discusses their implications, highlighting key findings. Finally, Section 4 concludes the study, summarizing the main contributions and offering directions for future research.

2. Problem Formulation and Methodology

This section presents the analytical formulation of reflection coefficients for the interactions of regular waves with a rectangular obstacle positioned at the bottom of the wave tank [18], as well as the interaction between water waves and a rectangular obstacle located at the free surface.

Based on this theoretical framework, we focus on the application of artificial intelligence (AI) to further analyze wave-structure interactions. Our strategy is to integrate these theoretical models with AI-driven methods to automate and optimize problem-solving processes (see Figure 1 below).

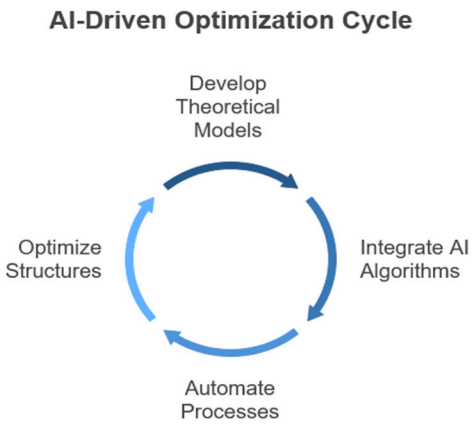

Figure 1. AI-driven optimization cycle.

For more clarity, we aim to use five machine-learning methods to investigate effective techniques for analyzing wave-structure interactions. Additionally, the datasets utilized in these machine-learning methods are derived from a theoretical approach that has already been validated in our latest research [18]. By training AI models on datasets generated from various wave conditions and breakwater configurations, we can identify patterns and relationships that may not be immediately apparent through traditional analytical methods. This approach not only enhances our understanding of wave dynamics but also enables us to predict performance outcomes for different design scenarios.

Furthermore, we will explore artificial intelligence (AI) techniques to refine breakwater design parameters, identifying optimal configurations that maximize wave attenuation while minimizing material costs and environmental impacts.

The theoretical formulation is divided into two parts. The first part addresses the expression of the reflection coefficient based on the conservation of flow rate and the continuity of velocity potential for wave-structure interactions cited at the bottom of the wave tank. The second part focuses on expressing the reflection coefficient for wave-structure interactions at the free surface.

2.1. Part 1: Wave-Structure Interactions Cited at the Bottom of Wave Tank

To theoretically analyze the interactions of waves with a rectangular structure located at the bottom of the wave tank (Figure 2 below), we establish an analytical formulation based on the conservation of flow rate and the continuity of velocity potential to express the reflection coefficient.

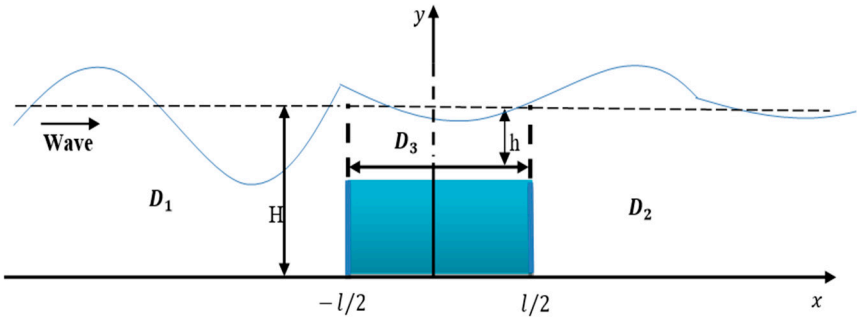

Figure 2. Configuration of bottom submerged breakwater (for analytical calculation).

The velocity potential for each subdomain is expressed as follows:

- At the subdomain D_1,

$$\phi_1 = a\left[exp\left(-jk(x+l/2)\right) + \mathrm{R}_b exp\left(jk(x+l/2)\right)\right] ch\left(k(y+H)\right), \quad (1)$$

- At the subdomain D_2,

$$\phi_2 = aT_b exp\left(-jk(x-l/2)\right) ch\left(k(y+H)\right), \quad (2)$$

- At the subdomain D_3,

$$\phi_3 = a[Cexp(-j\sigma x) + Dexp(j\sigma x)] ch\left(\sigma(y+h)\right). \quad (3)$$

The continuity flow rate conservation is defined at $x = -l/2$ and $x = l/2$ as follows:

- At the position $x = -l/2$,

$$\int_{-h}^{0} \phi_1(-l/2, y) ch\left(\sigma(y+h)\right) dy = \int_{-h}^{0} \phi_3(-l/2, y) ch\left(\sigma(y+h)\right) dy \quad (4)$$

$$\int_{-h}^{0} \frac{\phi_1(-l/2,y)}{\partial x} ch\left(k(y+H)\right) dy = \int_{-\mathrm{h}}^{0} \frac{\partial \phi_3(-\mathrm{l}/2,y)}{\partial \mathrm{x}} ch\left(k(y+H)\right) dy, \quad (5)$$

- At the position $x = l/2$,

$$\int_{-h}^{0} \phi_1(l/2, y) ch\left(\sigma(y+h)\right) dy = \int_{-h}^{0} \phi_3(l/2, y) ch\left(\sigma(y+h)\right) dy, \quad (6)$$

$$\int_{-h}^{0} \frac{\partial \phi_1(l/2,y)}{\partial \mathrm{x}} ch\left(k(y+H)\right) dy = \int_{-h}^{0} \frac{\partial \phi_3(l/2,y)}{\partial \mathrm{x}} ch\left(k(y+H)\right) dy, \quad (7)$$

Following the expression of the boundary conditions at the positions $x = l/2$ and $x = -l/2$, we obtain an algebraic system represented as follows:

$$\begin{cases} I_1(1+R) = I_2(Cz + D\bar{z}) \\ I_1 T_r = I_2(C\bar{z} + Dz) \\ kI_3(1-R) = \sigma I_1(Cz - D\bar{z}) \\ kI_3 T_r = \sigma I_1(C\bar{z} - Dz) \end{cases} \quad (8)$$

The system of Equation (8) is written in matrix form as follows:

$$\begin{bmatrix} \mathrm{A} & \mathrm{B} \\ \mathrm{B} & \mathrm{A} \end{bmatrix} \begin{bmatrix} T_b \\ 0 \end{bmatrix} = \begin{bmatrix} \overline{z^2} & 0 \\ 0 & z^2 \end{bmatrix} \begin{bmatrix} \mathrm{A} & \mathrm{B} \\ \mathrm{B} & \mathrm{A} \end{bmatrix} \begin{bmatrix} 1 \\ \mathrm{R}_b \end{bmatrix} \quad (9)$$

Then, the reflection and coefficients are expressed as follows:

$$\mathrm{R}_b = \frac{z^2 - \overline{z^2}}{\overline{z^2}\mathrm{B}/\mathrm{A} - z^2 \mathrm{A}/\mathrm{B}}, \quad (10)$$

where

$$\mathrm{A} = \frac{I_1}{I_2} + \frac{kI_3}{\sigma I_1} \quad (11)$$

$$B = \frac{I_1}{I_2} - \frac{kI_3}{\sigma I_1}. \quad (12)$$

$$I_1 = \int_{-h}^{0} ch\left(k(y+d)\right) ch\left(\sigma(y+d)\right) dy, \quad (13)$$

$$I_2 = \int_{-h}^{0} ch^2\left(\sigma(y+h)\right) dy, \quad (14)$$

$$I_3 = \int_{-h}^{0} ch^2\left(k(y+H)\right) dy, \quad (15)$$

2.2. Part 2: Wave-Structure Interactions Cited at the Free Surface of Wave Tank

To conduct a theoretical analysis of the interactions between waves and a rectangular structure positioned at the free surface of the wave tank (Figure 3 below), we develop an analytical formulation based on the conservation of flow rate and the continuity of velocity potential to determine the reflection coefficient.

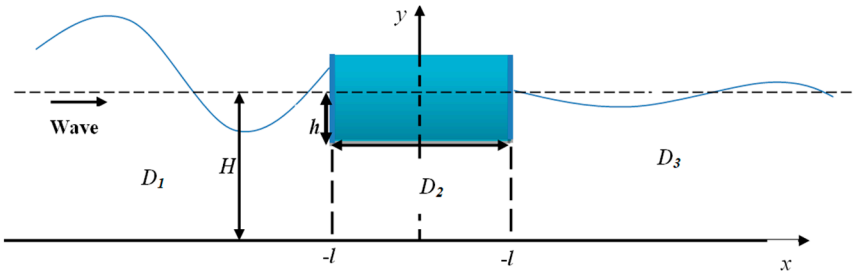

Figure 3. Configuration of free-surface submerged breakwater (for analytical calculation).

The velocity potential for each subdomain is expressed as follows:

- At the subdomain D1,

$$\varphi'_1(x,y,t) = a.\left(exp\left(-jk(x+l)\right) + R'.exp\left(jk(x+l)\right)\right).ch(ky).exp(j\omega t) \quad (16)$$

$$\varphi'_2(x,y,t) = \left(\frac{E'}{2} + \frac{F'}{2l}.x\right).exp(j\omega t) \quad (17)$$

$$\varphi'_3(x,y,t) = a.T'.exp\left(-jk(x-l)\right).ch(ky).exp(j\omega t) \quad (18)$$

Next, we express the continuity of potentials at $x = -l$ as follows:

$$\varphi'_1(-l,y) = \varphi'_2(-l,y) \quad (19)$$

$$\int_0^d \varphi'_1(-l,y)\,dy = \int_0^d \varphi'_2(-l,y)\,dy \quad (20)$$

$$(1+R')\int_0^d ch(ky).dy = \frac{1}{2}(E'-F')\int_0^d dy \quad (21)$$

$$E'-F' = 2(1+R')\frac{I'_1}{I''_2} \quad (22)$$

The flow rate conservation is expressed as follows:

$$\int_0^H \frac{\partial\varphi'_1(-l,y)}{\partial x}dy = \int_0^d \frac{\partial\varphi'_2(-l,y)}{\partial x}dy \quad (23)$$

$$jk(-1+R')\int_0^H ch(ky).dy = \frac{F'}{2l}\int_0^d dy \quad (24)$$

$$jk(-1+R')I'_3 = \frac{F}{2l}I'_2 \quad (25)$$

Further, we express the continuity of potentials at $x = l$ as follows:

$$\varphi'_3(l,y) = \varphi'_2(l,y) \quad (26)$$

$$\int_0^d \varphi'_2(l,y)\,dy = \int_0^d \varphi'_3(l,y)\,dy \quad (27)$$

$$\frac{1}{2}(E'+F')\int_0^d dy = T'\int_0^d ch(ky).dy \quad (28)$$

$$E'+F' = 2T'\frac{I'_1}{I'_2} \quad (29)$$

The flow rate conservation is expressed as follows:

$$\int_0^H \frac{\partial\varphi'_3(l,y)}{\partial x}dy = \int_0^d \frac{\partial\varphi'_2(l,y)}{\partial x}dy \quad (30)$$

$$\frac{F'}{2l}\int_0^d dy = -jkT'\int_0^H ch(ky).dy \quad (31)$$

$$\frac{F'}{2l}I'_2 = -jkT'I'_3 \quad (32)$$

Then, we obtain a system of equation as follows:

$$\begin{cases} E' - F' = 2(1 + R')\frac{I'_1}{I'_2} \\ E' + F' = 2T'\frac{I'_1}{I'_2} \\ jk(-1 + R')I'_3 = \frac{F'}{2l}I'_2 \\ \frac{F}{2l}I'_2 = -jkT'I'_3 \end{cases} \quad (33)$$

where

$$I'_1 = \int_0^{\mathrm{d}} ch(ky).dy = \frac{\sinh(kH(1-h/H))}{k} \quad (34)$$

$$I'_2 = \int_0^{\mathrm{d}} dy \quad (35)$$

$$I'_3 = \int_0^{\mathrm{H}} ch(ky).dy = \frac{\sinh(kH)}{k} \quad (36)$$

Finally, by combining the system of Equations (33), we obtain the reflection coefficient as follows:

$$R' = \frac{1}{1 - i\frac{\sinh(k(H-h))}{k.l.\sinh(KH)}} = \frac{1}{1 - i\frac{\sinh(kK(1-h/H))}{kH.(l/h).\sinh(KH)}} \quad (37)$$

Our study is structured into three key phases: (1) predicting the wave reflection coefficient based on the dimensions of a breakwater; (2) identifying the optimal height–width pair to achieve a desired level of reflection; and (3) extending this approach to a breakwater located at the free surface.

a. Data and Training Dataset Generation

To achieve these objectives, we used an analytical equation that models the reflection coefficient based on several parameters:

- KH: the relative water depth;
- h/H: the immersion ratio;
- l/H: the relative length;
- R_b: the reflection coefficient in the case of underwater breakwater;
- R': the reflection coefficient in the case of free-surface breakwater.

Based on this equation, we generated two primary datasets, each consisting of 32,000 data points:

- Underwater Breakwater: data representing various configurations of an obstacle submerged at the bottom of the wave tank;
- Free-Surface Breakwater: data for an obstacle located at the water's free surface, using similar parameters (h/H and l/H).

Each dataset was divided into 80% for training and 20% for testing. Additionally, 10,000 new data points were generated for a rigorous validation test, providing a total of 42,000 annotated data points for each case (underwater and free surface).

b. Choice and Justification of AI Algorithms

To model wave-structure interactions for both underwater and free-surface scenarios, we selected five AI algorithms based on their complementary features and suitability to the problem:

- Random Forest (RF) [34]: It was chosen for its ability to handle complex, nonlinear relationships between design parameters and the reflection coefficient. RF also provides variable importance, offering valuable insights into the influence of geometric parameters;

- Support Vector Regression (SVR) [35]: It is well-suited for multidimensional regression tasks, providing high accuracy in capturing the nuances of wave-structure interactions, even in complex configurations;
- Artificial Neural Network (ANN) [36]: Neural networks are well-suited for modeling nonlinear relationships, enabling the capture of subtle interactions between variables, essential for predicting wave reflection behavior;
- Decision Tree [37]: Its speed and interpretability make it an excellent choice for initial exploratory analysis. This model allows direct visualization of the impact of each parameter on the reflection coefficient;
- Gaussian Process (GP)[38]: This probabilistic model not only provides predictions but also confidence intervals, allowing the evaluation of result reliability—a valuable advantage in a maritime environment with variable conditions.

This diversity of algorithms allows us to cover a wide range of techniques, ensuring a thorough and accurate performance evaluation for each configuration.

c. Modeling Process and Performance Evaluation

The modeling process was carried out in two distinct steps:

i. Prediction of the Reflection Coefficient: In this first phase, the algorithms were trained to predict the reflection coefficients based on the parameters of the breakwater, including the submersion-to-height ratio (h/H), width (l/H), and relative water depth (KH). This phase validated the algorithms' ability to replicate the results of the analytical equation and accurately model wave-obstacle interactions;

ii. Prediction of the Optimal Height–Width Pair for a Given Reflection: In the second phase, the selected algorithm was used to reverse the initial reflection calculation and identify the optimal height–width pair (h/H, l/H) that met target reflection coefficients, effectively creating a "reciprocal function" of the analytical equation.

Each model configuration was carefully selected to optimize predictive accuracy and efficiency:

- Random Forest Regressor was configured with 100 estimators (Decision Tree) and a fixed random state of 42, ensuring reproducibility and robustness by averaging multiple decision tree outputs;
- Support Vector Regressor (SVR) used its default configuration to model complex, nonlinear relationships between input parameters and the reflection coefficient;
- Artificial Neural Network (ANN) was structured with two hidden layers of 50 neurons each and a maximum of 1000 iterations. ReLU activation was applied, along with a transformation to prevent negative outputs, ensuring the network accurately modeled the relationships while stabilizing training;
- Decision Tree Regressor was initialized with a random state of 42, allowing a single-tree model to capture relationships without ensembling, which makes the approach simpler and faster to train;
- Gaussian Process Regressor was employed to provide probabilistic predictions, modeling uncertainties in the reflection coefficient by assuming a Gaussian distribution of outputs.

Each model's performance was assessed based on Mean Squared Error (MSE), Root Mean Squared Error (RMSE), Mean Absolute Error (MAE), R^2, training duration, and prediction duration as mentioned in the Results Section. This rigorous approach, applied across both underwater and free-surface configurations, ensured robust and reliable optimization of breakwater dimensions under varying maritime conditions.

3. Results and Discussions

In this section, we present the performance of each artificial intelligence model used to predict the wave reflection coefficient and optimize the breakwater dimensions. The models were evaluated using several performance metrics to measure prediction accuracy, computational efficiency, and each model's ability to generalize under varying conditions. These metrics include Mean Squared Error (MSE), Root Mean Squared Error (RMSE), Mean Absolute Error (MAE), Coefficient of Determination (R^2), and the training and prediction durations. These parameters provide a comprehensive assessment of model quality, with each metric playing a specific role in judging the algorithms' suitability for accuracy and robustness in maritime environments.

3.1. Definitions and Utility of Performance Metrics

Each model's performance was assessed based on performance metrics below:

- Mean Squared Error (MSE): MSE calculates the average of the squared differences between predicted and actual values, penalizing larger errors more heavily. See Equation (38) below:

$$MSE = \frac{1}{n}\sum_{i=1}^{n}(y_i - \hat{y}_i)^2 \tag{38}$$

where

- y_i : actual value of the i-th data point;
- $\hat{y}_i$: predicted value of the i-th data point;
- n : number of data points.

In this study, MSE is used to evaluate each model's overall accuracy, particularly to identify those that minimize prediction errors.

- Root Mean Squared Error (RMSE): It is the square root of MSE. Using RMSE alongside MSE provides complementary insights into model performance. See Equation (39) below:

$$RMSE = \sqrt{MSE} \tag{39}$$

- Mean Absolute Error (MAE): MAE measures the average absolute difference between predictions and actual values (see Equation (40) below).

$$MAE = \frac{1}{n}\sum_{i=1}^{n}|y_i - \hat{y}_i| \tag{40}$$

While MSE gives more weight to larger errors, making it useful when large deviations are particularly undesirable, MAE offers a straightforward and robust alternative for assessing the average error magnitude without overemphasizing outliers.

- Coefficient of Determination (R^2): This score measures how well the predictions match the actual values, relative to the variance in the data. It is defined as follows:

$$R^2 = 1 - \frac{\sum_{i=1}^{n}(y_i - \hat{y}_i)^2}{\sum_{i=1}^{n}(y_i - \bar{y})^2} \tag{41}$$

where $\bar{y}$ is the mean of the actual values.

While MSE and MAE measure the magnitude of errors, R^2 adds value by providing a relative understanding of model performance compared to a baseline, such as always predicting the mean. R^2 is easier to interpret as it quantifies how much of the variation in the target variable is explained by the model. Additionally, it allows for comparison across datasets and helps detect overfitting when evaluated on different data splits.

- Training Time (TT): It refers to the duration required to train the model. It is measured as follows:

$$TT = t_{end} - t_{start} \tag{42}$$

where t_{start} and t_{end} are the timestamps indicating when training begins and ends, respectively.

This metric is important in our study as it determines whether a model can be quickly recalibrated when new data become available, a valuable asset in dynamic maritime applications.

- Prediction Time (PT): It refers to the time required to make predictions on new data. For a single input, it can be expressed as follows:

$$PT = t_{end} - t_{start} \tag{43}$$

where t_{start} and t_{end} are the timestamps indicating when prediction begins and ends, respectively.

This measure is crucial for real-time applications, where rapid predictions are necessary to adjust breakwater parameters in response to changing wave conditions.

By combining all these metrics, we obtain an overview of each model's performance, considering both accuracy and operational efficiency. This approach allows us to identify the models best suited for precise and fast predictions in a maritime environment.

3.2. Reflection Prediction

In this phase, we present the performance results of our proposed AI models for wave reflection prediction in underwater and free-surface breakwater.

Table 1 below shows the performance comparison of AI models for wave reflection prediction in underwater breakwater.

Table 1. Performance comparison of AI models for wave reflection prediction in underwater breakwater.

Model	MSE	RMSE	MAE	R^2	TT (s)	PT (s)
RF	6.25×10^{-8}	0.00025002	0.00011301	0.99999531	3.2104	0.1852
SVR	4.43×10^{-3}	0.06658152	0.05894506	0.66763488	2.446	0.3195
ANN	8.11×10^{-5}	0.00900543	0.00536504	0.99391981	2.9037	0.0079
DT	1.02×10^{-7}	0.00032000	0.00018931	0.99999232	0.083	0.005
GP	1.49×10^{-5}	0.00386001	0.00235702	0.99888291	215.006	60.685

In predicting wave reflection for underwater breakwaters, Random Forest (RF) and Decision Tree (DT) models provided the best balance of accuracy and efficiency. Both models achieved near-perfect fit, with extremely low error metrics (MSE, RMSE, and MAE) and high R^2 scores, indicating excellent predictive capability. Decision Tree further stood out with the fastest training and prediction times, making it highly efficient and suitable for real-time applications.

The Artificial Neural Network (ANN) also showed high accuracy, with the fastest prediction times among all models, making it ideal for scenarios requiring rapid predictions. However, it exhibited a slight overestimation near peak values, which may benefit from further tuning.

Gaussian Process (GP) was highly accurate but suffered from long training and prediction times, limiting its practicality to small datasets or offline analysis where computational time is less critical.

Support Vector Regressor (SVR) showed the weakest accuracy, with relatively high errors and lower R^2, making it unsuitable without further optimization. In summary, Random Forest, Decision Tree, and ANN are the most effective models for wave reflection prediction in underwater breakwater settings, balancing high accuracy with practical computational efficiency.

Moving from underwater to free-surface conditions, we next evaluate the performance of these AI models for wave reflection prediction in a free-surface breakwater context.

Table 2 below shows the performance comparison of AI models for wave reflection prediction in free-surface breakwater.

Table 2. Performance comparison of AI models for wave reflection prediction in free-surface breakwater.

Model	MSE	RMSE	MAE	R^2	TT (s)	PT (s)
RF	9.07×10^{-8}	0.00030116	0.00010446	0.999996963	3.5724	0.1968
SVR	4.30×10^{-3}	0.06560362	0.05871522	0.855901961	0.7296	0.0282
ANN	6.11×10^{-5}	0.00781446	0.00471538	0.997955438	3.6293	0.0115
DT	1.97×10^{-7}	0.00044414	0.00019752	0.999993396	0.0949	0.0055
GP	1.48×10^{-7}	0.00038483	0.00019241	0.999995042	212.3107	60.3129

Based on these results, we can observe that Random Forest, Decision Tree, and ANN maintain consistent performance across both breakwater settings, making them reliable choices for wave reflection prediction. SVR performs slightly better and faster in the free-surface environment, while the Gaussian Process remains accurate but computationally expensive in both.

These results suggest that while model accuracy remains largely stable across environments, computational efficiency may vary slightly, particularly for SVR and ANN in the free-surface context.

To visually reinforce these performance results, we present comparison curves that highlight the predictive accuracy of each AI model across varying values of the dimensionless parameter KH. Each curve represents the predictions from one of the five AI models—Random Forest, Support Vector Regressor (SVR), Artificial Neural Network (ANN), Decision Tree, and Gaussian Process—alongside the theoretical model.

These comparisons were based on a test dataset of 10,000 data points reserved specifically for validation. This extensive test set allows for a robust assessment of each model's ability to approximate the theoretical reflection behavior, providing a clear visual representation of each model's strengths and limitations relative to the analytical solution.

The graphs below show a validation test for underwater reflection, comparing theoretical model values (from an analytical equation) with predictions from various AI algorithms—Random Forest, SVR (Support Vector Regression), ANN (Artificial Neural Network), Decision Tree, and Gaussian Process. This test uses fixed values which were not present during the training or performance testing. It emphasizes the importance of model selection, particularly when extrapolating previously unseen data.

Here are the plots comparing the analytical reflection values with the predictions from each AI algorithm for different obstacle dimensions (h/H and L). See Figure 4 below (plots from a to d).

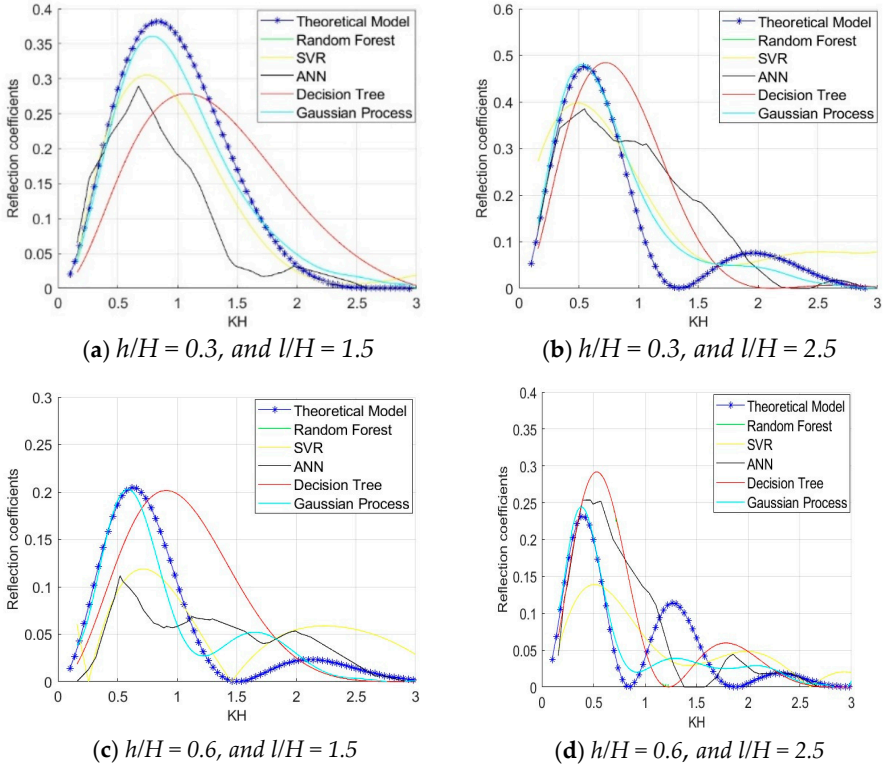

(**a**) *h/H = 0.3, and l/H = 1.5* (**b**) *h/H = 0.3, and l/H = 2.5*

(**c**) *h/H = 0.6, and l/H = 1.5* (**d**) *h/H = 0.6, and l/H = 2.5*

Figure 4. Plots comparing the analytical reflection values with the predictions from AI algorithms for different obstacle dimensions (h/H and l/H).

The discussion across all scenarios highlights consistent performance trends among the models evaluated for underwater reflection. Decision Tree (DT) and Random Forest (RF) capture the overall trend of reflection R effectively, particularly in the first harmonic (low KH), but struggle to model complex oscillations in intermediate and higher harmonics. Their rigid, "step-like" predictions show increasing deviations from the analytical equation as KH increases, with RF's lack of diversity in trees limiting its potential advantage over DT. Similarly, Support Vector Regression (SVR) captures the general trend but exhibits rigidity and produces non-physical negative values in some regions (h/H = 0.6, L1.5 and KH > 1.5, or h/H = 0.6 L = 2.5 and KH > 2.5) which was corrected using absolute values. These corrections ensured realistic outputs but introduced distortions in the oscillation structure. Artificial Neural Network (ANN) effectively models simple trends but fails to align peaks and troughs in more complex oscillations, sometimes producing artificial or misaligned variations due to suboptimal architecture or training.

Gaussian Process (GP) consistently outperforms all other models, offering high accuracy and fidelity across the scenarios tested in this study. It closely follows the analytical curve in all harmonics, capturing both global trends and fine oscillations, even in regions with rapid and dynamic variations. GP's flexibility allows it to model continuous transitions and complex interactions between waves and obstacles, with only minor deviations in extreme cases observed within the scope of the test conditions. This makes it the most reliable model for wave-obstacle interactions within the limits of this study, whereas the other models, although suitable for capturing general trends, require significant adjustments to handle complex and oscillatory behaviors effectively.

In the other case, Figure 5 shows a validation test for free-surface reflection, comparing theoretical model values (from an analytical equation) with predictions from various AI algorithms (RF, DT, SVR, GP, and ANN). See Figure 5 below (plots from a to d).

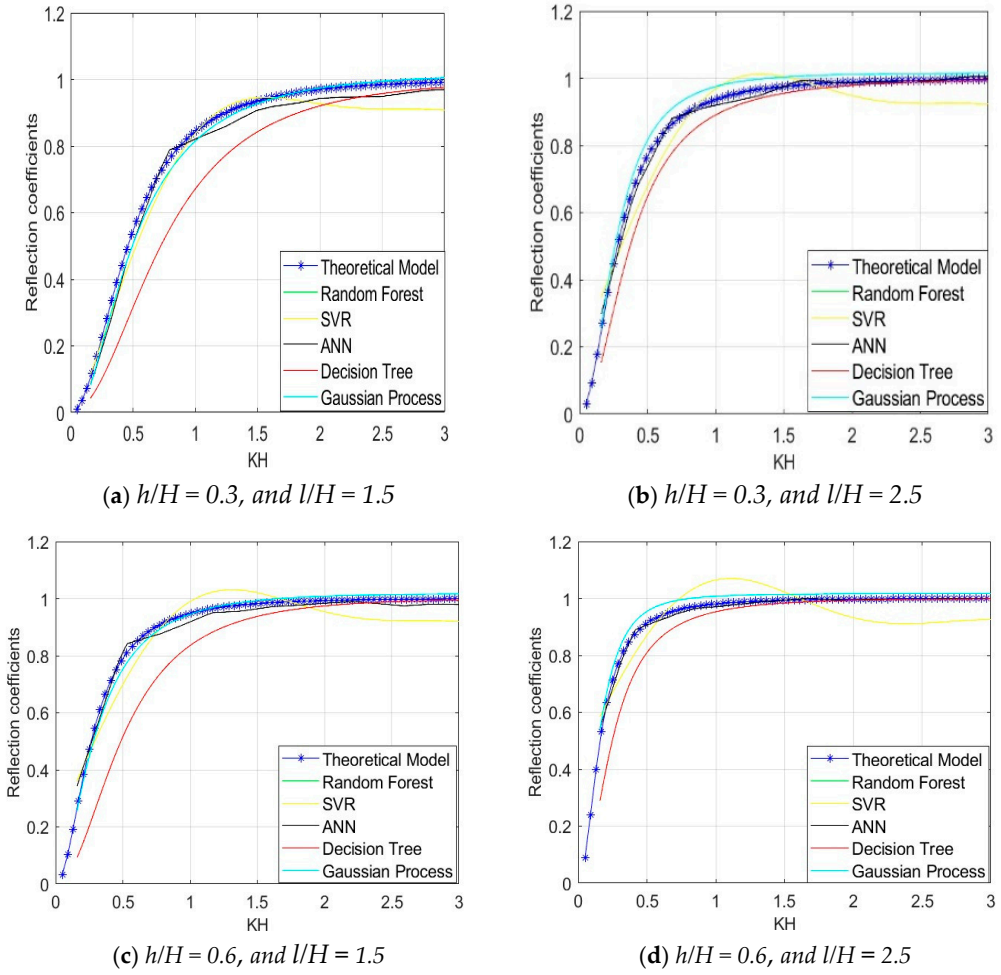

(**a**) *h*/*H* = 0.3, *and l*/*H* = 1.5 (**b**) *h*/*H* = 0.3, *and l*/*H* = 2.5

(**c**) *h*/*H* = 0.6, *and l*/*H* = 1.5 (**d**) *h*/*H* = 0.6, *and l*/*H* = 2.5

Figure 5. Plots comparing the analytical reflection values with the predictions from AI algorithms for different obstacle dimensions (h/H and l/H).

Across the four scenarios, the performance of the predictive models in replicating the analytical reference for wave reflection varies significantly. Decision Tree (DT) and Random Forest (RF) consistently capture general trends but exhibit notable deviations in regions with rapid variations in the reflection coefficient R, particularly for KH < 1.5 or in regions of complex relationships. Their comparable performances suggest limitations in the RF model's optimization or training data coverage. Gaussian Process (GP) demonstrates strong alignment in areas with gradual R variations and dense data coverage, but its predictions falter in regions with complex nonlinearities or sparse data. Notably, GP frequently exceeds the physical limit R = 1 in several scenarios, indicating the need for constraints to enforce physical consistency.

Support Vector Regression (SVR) exhibits acceptable predictions in some regions but shows significant deviations in others, often exceeding R = 1 or failing to generalize well for KH > 1.7. Its sensitivity to hyperparameters and lack of inherent physical constraints hinder its reliability. In contrast, the Artificial Neural Network (ANN) consistently emerges as the most robust and reliable model across all scenarios, maintaining minimal deviations and a strong alignment with the analytical reference throughout the entire range of KH. While some models benefit from improvements in hyperparameters, data enrichment, and kernel or architecture selection, ANN stands out as the most effective approach for accurately modeling wave reflection, combining flexibility with physical coherence.

3.3. Dimensions Prediction

In this phase, we present the performance results of our proposed AI models for the prediction of obstacle dimensions in underwater and free-surface cases.

Table 3 below shows the performance comparison of AI models for the prediction of obstacle dimensions in the underwater case.

Table 3. Performance comparison of AI models for the prediction of obstacle dimensions for underwater breakwater.

Model	Target	MSE	RMSE	MAE	R^2	TT (s)	PT (s)
RF	h/H	0.002955	0.054363	0.017301	0.928489	3.271199	0.077791
	l/H	0.092398	0.30397	0.110707	0.861997	4.188477	0.093852
DT	h/H	0.006158	0.078474	0.016343	0.850993	0.04668	0.002157
	l/H	0.165272	0.406537	0.109399	0.753153	0.062463	0.002334
SVR	h/H	0.025798	0.160617	0.129903	0.375774	26.310649	3.836463
	l/H	0.607661	0.779526	0.653736	0.092411	34.439204	5.889853
GP	h/H	0.022301	0.149336	0.117598	0.460379	244.665434	68.324839
	l/H	0.449268	0.670274	0.555867	0.328984	239.60938	68.330051
ANN	h/H	0.021895	0.147971	0.113052	0.470201	11.363988	0.013058
	l/H	0.414486	0.643806	0.51954	0.380934	195.429634	0.03317

The results show that Random Forest (RF) is the best-performing model, combining high accuracy (R^2 = 0.928 for h/H and 0.862 for L) with reasonable computational efficiency. Decision Tree (DT), while less accurate (R^2 = 0.851 for h/H), is highly efficient and serves as a viable alternative when resources are limited. In contrast, Support Vector Regression (SVR) and Gaussian Process (GP) deliver poor accuracy and are computationally expensive, making them unsuitable. Artificial Neural Network (ANN) shows moderate accuracy but higher computational demands, limiting its practicality.

Moving from underwater to free-surface conditions, we next evaluate the performance of these AI models for obstacle dimension prediction in a free-surface context.

Table 4 below shows the performance comparison of AI Models for the prediction of obstacle dimensions in a free-surface case.

Table 4. Performance comparison of AI models for the prediction of obstacle dimensions in a free-surface case.

Model	Target	MSE	RMSE	MAE	R^2	TT (s)	PT (s)
RF	h/H	0.001825	0.042724	0.012152	0.956379	3.781168	0.072074
	l/H	0.029419	0.171519	0.049657	0.95551	3.681144	0.073746
DT	h/H	0.003793	0.061584	0.013919	0.909367	0.058323	0.002116
	l/H	0.059431	0.243784	0.052862	0.910123	0.054024	0.002139
SVR	h/H	0.026049	0.161396	0.138118	0.377508	31.094358	4.719603
	l/H	0.422047	0.649651	0.526329	0.361739	36.449994	6.32239
GP	h/H	0.013696	0.117029	0.086317	0.672708	270.447472	68.376187
	l/H	0.371135	0.609208	0.48067	0.438733	247.67819	68.148208
ANN	h/H	0.017425	0.132003	0.103471	0.583595	20.12097	0.014777
	l/H	0.395293	0.628723	0.515053	0.402199	24.952677	0.015778

In free-surface conditions, Random Forest (RF) remains the best-performing model, achieving the highest accuracy (R^2 = 0.956 for both h/H and L) with reasonable computation times. Decision Tree (DT) offers a good trade-off between accuracy (R^2 = 0.909) and efficiency, making it ideal for resource-limited scenarios. In contrast, Support Vector Regression (SVR) and Gaussian Process (GP) perform poorly with low accuracy and high

computational costs, while Artificial Neural Network (ANN) provides moderate accuracy but is less practical due to higher training times.

4. Conclusions

This paper investigates the interaction between waves and two types of wave attenuators: a free-surface breakwater and an underwater breakwater fixed to the bottom of a channel. The focus of the study is the variation in the reflection coefficient as a function of the dimensionless parameter KH. Our findings indicate that the free-surface breakwater acts as a low-pass filter, with its reflective power increasing as its length grows and its immersion decreases. In contrast, the underwater breakwater exhibits a reflection curve that peaks before decreasing for shorter wavelengths, functioning as a band-pass filter. The study further reveals that the reflective power of the underwater breakwater intensifies with its length, with its most effective wave attenuation occurring at shallow immersion depths.

Additionally, this research highlights the transformative potential of machine learning (ML) in optimizing the design of both submerged and free-surface rectangular breakwaters. Utilizing five AI algorithms—Random Forest, Support Vector Regression, Artificial Neural Network, Decision Tree, and Gaussian Process—we successfully predicted wave reflection coefficients and determined optimal dimension ratios (h/H and L) for achieving specific wave behavior targets. The results demonstrate that Random Forest and Decision Tree offer a favorable balance between accuracy and computational efficiency, while Gaussian Process, though highly accurate, requires more computational resources. These findings emphasize the potential of AI to complement traditional approaches, offering a robust framework for addressing complex maritime engineering challenges. Future research should aim to refine these models, integrate additional environmental factors, and explore hybrid methodologies that combine multiple algorithms, ultimately improving predictive accuracy and enhancing the design of sustainable, cost-effective coastal defense systems.

Author Contributions: Conceptualization, M.L., S.E.M. and K.K.; methodology, M.L., S.E.M. and K.K.; software, M.L., S.E.M. and K.K.; validation, M.L., S.E.M. and K.K.; formal analysis, M.L., S.E.M. and K.K.; investigation, M.L., S.E.M. and K.K.; resources, M.L., S.E.M. and K.K.; writing—original draft preparation, M.L., S.E.M. and K.K.; writing—review and editing, M.L., S.E.M. and K.K.; visualization, M.L., S.E.M. and K.K.; supervision, M.L., S.E.M. and K.K.; project administration, M.L., S.E.M. and K.K.; funding acquisition, M.L., S.E.M. and K.K. All authors have read and agreed to the published version of the manuscript.

Funding: This research was founded by TUKE by the Ministry of Education, Science, Research and Sport of the Slovak Republic.

Data Availability Statement: Data is contained within the article.

Acknowledgments: The paper presented was supported by the project VEGA 1/0307/23 of the Scientific Grant Agency of the Ministry of Education, Science, Research and Sport of the Slovak Republic.

Conflicts of Interest: The authors declare no conflict of interest.

Nomenclature

a	The amplitude of the incident wave
R_b	The reflection coefficient in the case of bottom breakwater
R'	The reflection coefficient in the case of free-surface breakwater
T_b	The transmission coefficient in the case of bottom breakwater

ϕ	Velocity potential in the case of bottom breakwater study
φ'	Velocity potential in the case of free-surface breakwater study
d = H − h	The height under the obstacle in the case of free-surface breakwater
T'	The transmission coefficient
H	The water depth at D_1 and D_2 locations
h/H	The immersion ratio
l/H	The relative length
KH	The relative water depth
k	The wave number that verifies the dispersion relation $\frac{\omega^2}{g} = kth(kH)$
σ	The wave number above of the obstacle that verifies the dispersion relation $\frac{\omega^2}{g} = \sigma\, th(\sigma h)$

References

1. Zhang, C.; Lu, Y. Study on artificial intelligence: The state of the art and future prospects. *J. Ind. Inf. Integr.* **2021**, *23*, 100224.
2. Haleem, A.; Javaid, M.; Qadri, M.A.; Singh, R.P.; Suman, R. Artificial intelligence (AI) applications for marketing: A literature-based study. *Int. J. Intell. Netw.* **2022**, *3*, 119–132.
3. Castiglioni, I.; Rundo, L.; Codari, M.; Di Leo, G.; Salvatore, C.; Interlenghi, M.; Gallivanone, F.; Cozzi, A.; D'Amico, N.C.; Sardanelli, F. AI applications to medical images: From machine learning to deep learning. *Phys. Medica* **2021**, *83*, 9–24.
4. Spanaki, K.; Karafili, E.; Despoudi, S. AI applications of data sharing in agriculture 4.0: A framework for role-based data access control. *Int. J. Inf. Manag.* **2021**, *59*, 102350.
5. Rajpurkar, P.; Chen, E.; Banerjee, O.; Topol, E.J. AI in health and medicine. *Nat. Med.* **2022**, *28*, 31–38.
6. Taebi, A. Deep learning for computational hemodynamics: A brief review of recent advances. *Fluids* **2022**, *7*, 197.
7. Cravero, C.; De Domenico, D.; Marsano, D. The use of uncertainty quantification and numerical optimization to support the design and operation management of air-staging gas recirculation strategies in glass furnaces. *Fluids* **2023**, *8*, 76.
8. Brunone, B.; Maietta, F.; Capponi, C.; Duan, H.-F.; Meniconi, S. Detection of partial blockages in pressurized pipes by transient tests: A review of the physical experiments. *Fluids* **2023**, *8*, 19.
9. Karakasidis, T.E.; Sofos, F.; Tsonos, C. The electrical conductivity of ionic liquids: Numerical and analytical machine learning approaches. *Fluids* **2022**, *7*, 321.
10. Holmes, W.; Tuomi, I. State of the art and practice in AI in education. *Eur. J. Educ.* **2022**, *57*, 542–570.
11. Wang, S.; Zhang, Y.; Zhang, X.; Gao, Z. A novel maritime autonomous navigation decision-making system: Modeling, integration, and real ship trial. *Expert Syst. Appl.* **2023**, *222*, 119825.
12. Tsai, C.-M.; Lai, Y.-H.; Perng, J.-W.; Tsui, I.-F.; Chung, Y.-J. Design and application of an autonomous surface vehicle with an AI-based sensing capability. In Proceedings of the 2019 IEEE Underwater Technology (UT), Taiwan, China, 16–19 April 2019 IEEE: New York, NY, USA, 2019; pp. 1–4.
13. Chae, C.-J. The Evolution of Maritime Technology Development: A Dynamic Positioning System Perspective of Maritime Autonomous Surface Ship. *WMU J. Marit. Aff.* **2024**, 1–29.
14. Qiao, Y.; Yin, J.; Wang, W.; Duarte, F.; Yang, J.; Ratti, C. Survey of deep learning for autonomous surface vehicles in marine environments. *IEEE Trans. Intell. Transp. Syst.* **2023**, *24*, 3678–3701.
15. Jimenez, V.J.; Bouhmala, N.; Gausdal, A.H. Developing a predictive maintenance model for vessel machinery. *J. Ocean Eng. Sci.* **2020**, *5*, 358–386.
16. Carraro, M.; De Vanna, F.; Zweiri, F.; Benini, E.; Heidari, A.; Hadavinia, H. CFD modeling of wind turbine blades with eroded leading edge. *Fluids* **2022**, *7*, 302.
17. Tay, Z.Y.; Hadi, J.; Chow, F.; Loh, D.J.; Konovessis, D. Big data analytics and machine learning of harbour craft vessels to achieve fuel efficiency: A review. *J. Mar. Sci. Eng.* **2021**, *9*, 1351.
18. Loukili, M.; Dutykh, D.; Nadjib, C.; Ning, D.; Kotrasova, K. Analytical and numerical investigations applied to study the reflections and transmissions of a rectangular breakwater placed at the bottom of a wave tank. *Geosciences* **2021**, *11*, 430. https://doi.org/10.3390/geosciences11100430.
19. Dean, W.R. On the reflexion of surface waves by a submerged plane barrier. *Math. Proc. Camb. Philos. Soc.* **1945**, *41*, 231–238.
20. Takano, K. Effets d'un obstacle parallélépipédique sur la propagation de la houle. *Houille Blanche* **1960**, *3*, 247–267.

21. Patarapanich, M. Forces and moment on a horizontal plate due to wave scattering. *Coast. Eng.* **1984**, *83*, 279–301.
22. Liu, P.L.F.; Wu, J. Wave transmission through submerged apertures. *J. Waterw. Port Coast. Ocean Eng.* **1987**, *113*, 660–671.
23. Stamos, D.J.; Hajj, M.R.; Telionis, D.P. Performance of hemi-cylindrical and rectangular submerged breakwaters. *Ocean Eng.* **2003**, *30*, 813–828.
24. Molin, B.; Kimmoun, O.; Liu, Y.; Remy, F.; Bingham, H.B. Experimental and numerical study of the wave run-up along a vertical plate. *J. Fluid Mech.* **2010**, *654*, 363–386.
25. Liu, Y.; Li, H.J.; Zhu, L. Bragg reflection of water waves by multiple submerged semi-circular breakwaters. *Appl. Ocean Res.* **2016**, *11*, 67–78.
26. Scyphers, S.B.; Powers, S.P.; Heck, K.L. Ecological Value of Submerged Breakwaters for Habitat Enhancement on a Residential Scale. *Environ. Manag.* **2015**, *55*, 383–391.
27. Mei, C.; Black, J. Scattering of surface waves by rectangular obstacles in waters of finite depth. *J. Fluid Mech.* **1969**, *38*, 499–511.
28. Massel, S. Harmonic generation by waves propagating over a submerged step. *Coast. Eng.* **1983**, *7*, 357–380.
29. Driscoll, A.; Dalrymple, R.; Grilli, S. Harmonic generation and transmission past a submerged rectangular obstacle. *Coast. Eng.* **1992**, 1142–1152.
30. Szmidt, K. Finite difference analysis of surface wave scattering by underwater rectangular obstacles. *Arch. Hydro-Eng. Environ. Mech.* **2010**, *57*, 179–198.
31. Akoz, M.S.; Cobaner, M.; Kirkgoz, M.S.; Oner, A.A. Prediction of geometrical properties of perfect breaking waves on composite breakwaters. *Appl. Ocean Res.* **2011**, *33*, 178–185.
32. Kuntoji, G.; Rao, M.; Rao, S. Prediction of wave transmission over submerged reef of tandem breakwater using PSO-SVM and PSO-ANN techniques. *ISH J. Hydraul. Eng.* **2020**, *26*, 283–290.
33. Mao, P.; Chen, C.; Chen, X.; Zhang, Q.; Bao, Y.; Yang, Q. An innovative design for floating breakwater with Multi-objective genetic optimal method. *Ocean Eng.* **2024**, *312*, 119202.
34. Breiman, L. Random forests. *Mach. Learn.* **2001**, *45*, 5–32.
35. Drucker, H. B.; Christopher, J.; Kaufman, L.; Smola, A.; Vapnik, V. Support vector regression machines. In *Advances in Neural Information Processing Systems*; MIT Press: Cambridge, MA, USA, 1996; p. 9.
36. Zupan, J. Introduction to artificial neural network (ANN) methods: What they are and how to use them. *Acta Chim. Slov.* **1994**, *41*, 327.
37. Quinlan, J.R. Learning decision tree classifiers. *ACM Comput. Surv. (CSUR)* **1996**, *28*, 71–72.
38. Mackay, D.J.C. Introduction to Gaussian processes. In *NATO ASI Series F Computer and Systems Sciences*; Springer Verlag: Berlin/Heidelberg, Germany, 1998; Volume 168, pp. 133–166.